FUDMA Journal of Sciences (FJS)
ISSN online: 2616-1370
ISSN print: 2645 - 2944
Vol. 9 No. 12, December (Special Issue), 2025, pp 247 – 255
DOI: https://doi.org/10.33003/fjs-2025-0912-4182

PHYSIOCHEMICAL, THERMAL, AND MORPHOLOGICAL CHARACTERISTICS OF MILLET HUSK (*PENNISETUM GLAUCUM L*) FOR POLYMER COMPOSITE APPLICATION

***Aliyu Isah, Shaibu Lasisi and Rufai Dahiru**

Department of Metallurgical Engineering, Waziri Umaru Federal Polytechnic, Birnin Kebbi, 1034, Nigeria

*Corresponding authors' email: engalisa@yahoo.com

ABSTRACT

The depletion of synthetic fibers, which are mostly petroleum-based products, has mitigated the growing need to search for natural fibers for local and industrial applications. There is a need to identify new natural fibers for utilization in polymer matrix composites in order to achieve a better mix of fiber and polymer for a variety of applications. Therefore, this research aims to characterize untreated and alkaline-treated millet husk (*Pennisetum glaucum L*) as an underexplored fiber to evaluate its physiochemical and thermal behaviour for its possible use as reinforcement in a polymer matrix. Millet husk is a waste obtained after threshing and separation of millet grains from the panicle with fruit of the millet plant. The findings revealed that the alkali-treated millet husk (TMH) contains higher cellulose content of 73.74 %, lower density of 0.10 g/cm^3, less moisture content of 1.37 %, and higher crystallinity index (CI) of 66.67 % than untreated millet husk (UTMH). There was a disappearance of the lignin peak in Fourier transform infrared (FTIR) and an improvement in thermal degradation temperature of the TMH. The surface morphology of TMH was found to be rough, which enables effective adhesion with the polymer matrix. Thus, the improved properties of TMH demonstrate its utilization as a possible reinforcement material in the development of polymer composites.

Keywords: Millet husk, Alkali treatment, Physical properties, Chemical properties, Thermal behaviour

INTRODUCTION

Synthetic fibers have been used over the years for the development of polymer composites. The polymer composites developed from synthetic fiber are associated with a negative effect on the environment by their non-degradability, which pollutes the environment and causes health hazards. Synthetic fibers, which are petroleum products diminished gradually due to their high weight, high cost, and limited supply, a major setback for the fabrication of composite material (Ikumapayi et al., 2022). Over ten years ago, natural fibers were the preferred choice over synthetic fibers employed as reinforcing material in polymer composites due to their economic benefit to the environment. The increased need for sustainable materials has resulted in a paradigm shift toward using natural fibers rather than synthetic fibers in the production of polymer composites (Kumar et al., 2019). The increased demand globally for the utilization of sustainable development goals has led researcher's enthusiasm for the usage of natural fibers as raw materials for technological advancement (Acharya et al., 2024; Rao et al., 2024). Natural fiber have gained popularity in recent times because of their high concentrations of cellulose, pectin, lignin, ash, hemicellulose, wax, and low moisture content, and they are widely employed due to their light light, high toughness, flexibility in bending, nontoxic nature, biodegradability behaviour, reasonable specific strength, and cost-effectiveness (Eyupoglu et al., 2024; Karimah et al., 2021; Kusuma et al., 2024). However, the properties of natural fiber differ according to the species, growing habitat, fiber processing technique, and geographical location (Sanyang et al., 2016). However, natural fibers have some disadvantages when employed in the fabrication of polymer composites, such as substantial changes in characteristics, poor moisture absorption, and swelling behaviour, which cause cracks and increase material flaws (Al-Maharma & Al-Huniti, 2019). Furthermore, poor bonding of natural fibers with various polymer matrices occurred due to hydrophilic and hydrophobic qualities, resulting in another disadvantage (Lee et al., 2021). These drawbacks are effectively corrected via surface modification techniques such as physical, chemical, or biological treatment to break the atomic bond of the fiber surface to enable its functionalization (Mohammadi et al., 2024). An estimated 1.78 × 109 tons of natural fiber are produced each year, and the natural fibers are categorized according to their source, including vegetable, animal, and mineral fibers (Thapliyal et al., 2023).

Millet is a widely consumed cereal grain in the world that belongs to the family of vegetable fibers. It is particularly popular in the semi-arid nations of Africa and Asia, which produce the most millet globally (Yousaf et al., 2021). Millet is the most often consumed staple food, with excellent storage properties, high nutritional content, disease resistance, and the ability to survive soil moisture stress (Bashir et al., 2022). The millet is covered with millet husk, which is extracted by dehusking the millet. As an agricultural waste, millet husk is typically burned and incinerated over time, releasing greenhouse gases that pose a potential danger to the environment. (Gairola et al., 2022). Furthermore, the millet husk stockpile in farmlands decomposes over time into manure, providing a habitat for microorganisms that cause disease. The decomposition of millet husk in farmlands produces methane gas, which is 21 times more detrimental to the ozone layer. As a result, the safest approach to dispose of millet husk is to use it as a possible reinforcement material because of its lightweight nature, renewability, ready availability, and biodegradability (Adazabra & Viruthagiri, 2023). For millet husk to be considered as a suitable reinforcement material in a polymer composite, its physiochemical characteristics, thermal behaviour, and morphological characteristics must be ascertained. Thus, the primary aim of this research is to investigate the physical characteristics (density and moisture content), chemical characteristics (XRD and FTIR), thermal behaviour, and morphological features of the alkali-treated millet husk and untreated millet husk (*Pennisetum glaucum L*) for possible utilization as reinforcing material in polymer composites production.

MATERIALS AND METHODS

Materials

The millet husk utilized in the research was sourced from a nearby local farm in Kalgo Village, Birnin Kebbi, Kebbi State, Nigeria, during the harvesting period between September to October of every year. Concentrated NaOH solution was purchased from Kinzoo Chemical Shop, Zaria, Kaduna State, Nigeria.

Preparation of Millet Husk

Millet husk of 500 g was collected from the millet plant panicle with fruits (Figure 1a) after the dislodging of millet grains via threshing. After collecting the millet husk (Figure 1b), it was thoroughly washed with clean tap water to remove any dirt, contaminants, and stones. It was then allowed to dry in the lab for 2 days. To further remove any retained moisture, the millet husk was then dried for 24 h at 75 ˚C in an electric oven. Thereafter, the dried millet husk was milled to produce powdered untreated millet husk (UTMH) (Figure 1c) and stored in a polymer bag at room temperature for characterization.

Treatment of Millet Husk with NaOH Solution

Alkali treatment was carried out by soaking 100 g of the dried millet husk in 500 ml of 3 % NaOH solution for 24 h at room temperature. The soaked millet husk after 24 h in 3 % NaOH solution was properly stirred and followed by washing repeatedly with distilled water to completely wash out the alkali (NaOH) solution. The washed and treated millet husk (TMH) (Figure 1d) was further dried in the laboratory for 24 h and subsequently dried in an electric oven set to 75 ˚C for another 24 h to eliminate any remaining moisture.

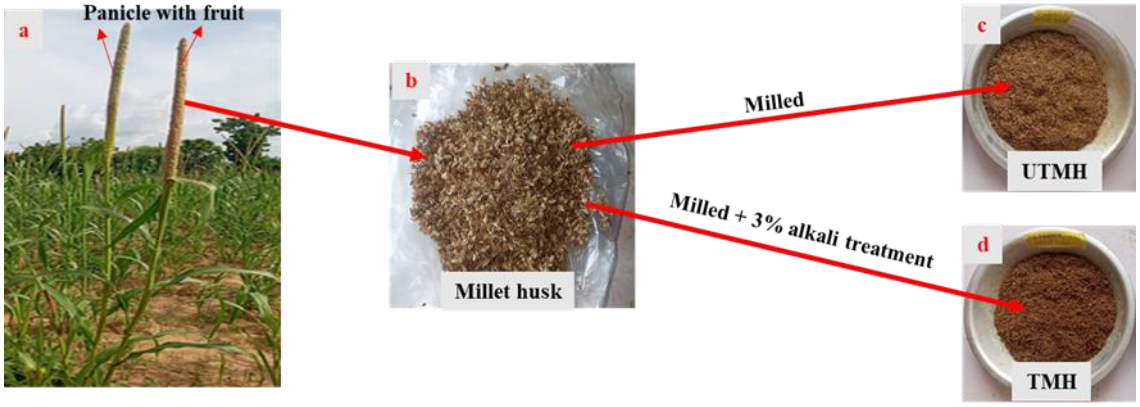

Figure 1: Millet husk preparation from (a) panicle with fruit, (b) millet husk, (c) UTMH, and (d) TMH

Characterization of UTMH and TMH

Determination of Chemical Composition of UTMH and TMH

The method used by Ilyas et al., (2021) was followed in determining the chemical compositions of TMH and UTMH. In this technique, lignin, acid detergent fiber (ADF), and neutral detergent fiber (NDF) of both the UTMH and TMH were determined. Furthermore, the amount of hemicellulose and cellulose content was calculated using equations 1 and 2, respectively.

$$Hemicellulose = ADF - Lignin \quad (1)$$

$$Cellulose = NDF - ADF \quad (2)$$

Determination of Density of UTMH and TMH

The density of the UTMH and TMH was evaluated by first determining their respective mass and volume using a gas pycnometer (Norcross, GA, USA). The UTMH and TMH were dried in an oven heated to 75 ˚C for a period of 24 h to to derive off the retained moisture in the UTMH and TMH and then stored in a desiccator. The dried UTMH and TMH were placed in a pycnometer to determine both the mass and volume. From the determined mass and volume, the densities were calculated using equation (3).

$$Density = \frac{Mass\ (m)}{Volume\ (v)} \quad (3)$$

Determination of Moisture Content of UTMH and TMH

The UTMH and TMH samples were taken for the moisture content determination. A representative sample of UTMH and TMH were weighed before ($W_{initial}$) and after (W_{final}) being placed in an oven for 24 h at 75 ˚C using a digital weighing balance scale. The moisture content was then calculated using equation (4).

$$Moisture\ Content = \frac{W_{initial} - W_{final}}{W_{initial}} \times 100 \quad (4)$$

X-Ray Diffraction (XRD)

The X-ray diffraction patterns of UTMH and TMH samples were analyzed using an XRD machine (Shimadzu MiniFlex600-C) operating at AC 100 and 240 V with a wavelength of Cu-Kα, 1.5405 Å at a rate of 2 ˚/min within an angle range of 2θ = (4˚ – 90˚). Using peak height methods provided by Segal's analytical equation (5), the crystallinity index (CI) of the UTMH and TMH X-ray diffraction patterns was determined (Segal et al., 1959).

$$CI(\%) = \frac{I_{002} - I_{am}}{I_{002}} \times 100 \quad (5)$$

Where I_{am} is the intensity dispersed by the materials' amorphous phase, measured between 18˚ and 19˚, and I_{002} is the highest intensity of the (200) lattice peak of cellulose, situated at a diffraction angle of around 22˚ and 23˚.

Fourier Transform Infrared (FTIR) Spectroscopy

The functional groups present in UTMH and TMH samples were determined using an FTIR (Xenemetrix, IF, EX-2600/X-2600) spectrometer. The analysis was carried out by using 2.5 mg samples each mixed separately with a 1:100 ratio solution of KBr and moulded into a pellet with the assistance of a hydraulic press. A wavelength range of 4000-400 cm^{-1} region at 4 cm^{-1} with 16 scans FTIR spectrometer with altered total reflectance capacities was employed for the analysis to obtain

data. The analysis was carried out at room temperature and at normal atmospheric humidity.

Thermogravimetric Analysis (TGA)

The UTMH and TMH samples' thermal characteristics were analyzed with a Q500 V2A0.13 thermogravimetric analyzer (Bellingham, USA). A known mass of 10 mg of the samples were put in a platinum crucible, heated to a range of temperatures of 25 to 600 ˚C at 10 º/min in the presence of nitrogen gas supplied at a rate of 20 ml/min.

Scanning Electron Microscopy (SEM) Analysis

The Phenom Corem-EM-30AX+ SEM was used to analyze the morphological surface of the TMH and UTMH samples under ambient room conditions at an accelerating voltage of 5 kV. Aluminium stubs were employed to mount the UTMH and TMH samples with an adhesive double-sided tape. Furthermore, the UTMH and TMH samples were coated to prevent charging with a thin golden film of 0.1 μm. The sample's surface resolution was measured at 4.0 nm using BSE imaging in low vacuum mode.

RESULTS AND DISCUSSION

Chemical Composition Evaluation of UTMH and TMH

The most important plant constituents are made up of three major components, which are lignin, cellulose, and hemicellulose. The quantities of cellulose, hemicellulose, and lignin are major determinants of constituents that determine the characteristics of natural fibers (Adamu et al., 2024; Atalie & Gideon, 2018). The chemical constituents of the UTMH and TMH are presented in Table 1 and compared to other natural fibers investigated. The cellulose content of the UTMH and TMH was found to be 62.59 % and 73.74 %, respectively, as shown in Table 1. The cellulose content of the TMH increased by 15.12 % after treatment with 3 % NaOH compared to the UTMH. The natural fiber with high cellulose content, when used as a reinforcement material in a polymer composite, improves the mechanical characteristics (Morin et al., 2021). The cellulose contents of both UTMH and TMH were seen to be higher than some natural fibers, as shown in Table 1. The hemicellulose content of the UTMH (23.33 %) was seen to be lower than that of TMH (13.74 %) (See Table 1). The decrease in hemicellulose of TMH compared to that of UTMH could be a result of dissolution and washing away of the hemicellulose content. Furthermore, the lignin content of UTMH and TMH was found to be 5.38 % and 3.61 %, respectively, as it appears in Table 1. The lignin content of TMH was found to be lower than that of UTMH (See Table 1). The lower lignin content obtained with TMH could be due to the delignification process during NaOH dissolution. The presence of high amount of hemicellulose and lignin content in natural fiber poses detrimental consequences in terms of the properties of the composite when employed as reinforcement. The high value of hemicellulose and lignin content from a natural fibers render them hydrophilic which are not compactible with hydrophilic polymer matrix (Samanth & Bhat, 2023). The lignin content of UTMH and TMH were seen to be lower than that of arrowrrot husk fiber (AHF), pineapple leaf fiber (PLF), untreated sugarcane bagasse (UTSB), Treated sugarcane bagasse (TSB), corn husk (CH), and sisal fiber (SF), as showm in Table 1. The UTMH ash content of 0.19 % was found to be higher than that of of TMH (0.16 %). Consequently, the ash content of both UTMH and TMH were seen to be lower than some natural fibers, as seen in Table 1. High ash content above 2 % is disadvantageous in mechanical properties for the end product and not suitable for polymer matrix composite production (Wan Nadirah et al., 2012). As shown in Table 1, the moisture content of the TMH was found to be lower (1.37 %) compared to the UTMH (5.94 %) and other fibers, including sisal and arrowroot husk fiber. Higher moisture content in a fiber material when used as reinforcement in a polymer matrix results in lower mechanical properties compared to a fiber with low moisture content (Bachchan et al., 2022). In conclusion, NaOH treatment increases cellulose while decreasing lignin, hemicellulose, and ash content of natural fibers, as seen in Table 1.

Table 1: Physicochemical Characteristics of UTMH, TMH, and Other Fibers

Content	Cellulose (%)	Hemicellulose (%)	Lignin (%)	Ash (%)	Moisture Content (%)	Density (g/cm^3)	References
UTMH	62.59	23.33	5.38	0.19	5.94	0.12	Current work
TMH	73.74	13.77	3.61	0.16	1.37	0.10	Current work
AHF	37.35	26.85	8.89	8.79	5.51	1.23	(Tarique et al., 2022)
PLF	74.33	-	10.41	4.73	-	-	(Wan Nadirah et al., 2012)
UTSCB	45.00	32.13	19.01	5.01	5.01	-	(Hamin et al., 2023)
TSCB	71.00	13.04	7.01	8.02	8.09	-	(Hamin et al., 2023)
Sisal	73.53	10.02	8.00	1.50	12.23	1.66	(Bekele et al., 2022)
CH	45.70	35.80	4.03	0.35	7.81	1.49	(Ibrahim et al., 2019)

Densities Analysis of UTMH and TMH

The low density of natural fibers is one of the essential parameters that necessitate their selection to be employed as reinforcement material in the production of polymer matrix composites (Ilyas et al., 2018). The densitis of UTMH and TMH were found to be 0.12 g/cm^3 and 0.10 g/cm^3, respectively, and were observed to be lower than those of other natural fibers, such as arrowroot husk fiber (1.23 g/cm^3), sisal fiber (166 g/cm^3), and corn husk (1.49 g/cm^3), as shown in Table 1. The low-density values obtained for UTMH and TMH signify their potential application for the fabrication of light-weight biocomposites. This characteristic of lower densities possessed by natural fibers (Table 1) makes then more attractive for the development of lightweight polymer composite as reinforcement compared to synthetic reinforcement, such as E-glass fiber with a density of 2.54 g/cm^3 (Paramasivam et al., 2024; Rao et al., 2023).

XRD Analysis of UTMH and TMH

XRD analysis was carried out to ascertain the X-ray diffraction pattern and percentage crystallinity index of UTMH and TMH. The XRD pattern of the UTMH and TMH, revealing their respective peaks and crystallinity index, is represented in Figure 2. The XRD patterns of UTMH and TMH were characterized with strong peaks at 21.38˚ and 21.22˚, respectively, and a weak peak of 16.72˚ for TMH. The confirmation of the cellulosic content of the material is seen with the appearance of sharp peaks of well-ordered crystalline

peaks (Huang et al., 2019). The crystallinity index of UTMH and TMH of 48.17 % and 66.67 %, respectively, was obtained, as shown in Figure 2 and Table 2. Table 2 displays the resultant crystallinity index of UTMH and TMH in comparison to recently published work using different extraction routes. The crystallinity index of UTM was found to be higher than that of UTMH, making TMH to be more higher in strength compared to UTMH. The low concentration of amorphous non-cellulosic components, such as hemicellulose and lignin, which are eliminated by alkali treatment, explains why THM has a greater crystallinity index value than UTMH (Abdul Karim et al., 2023). It has been found that natural fibers with a high crystallinity index value, when used as a reinforcing material in biocomposite production, results in a rigid structure (Sánchez-Safont et al., 2018).

Table 2: Comparison of Natural Fibers Crystallinity Index values with Extraction Techniques

Natural fibers	Extraction Techniques	Crystallinity Index (%)	References
Goosegrass	Manual milling	45.00	(Khan et al., 2021)
Sugarcane bagasse	Mechanical milling	52.17	(Sankhla et al., 2021)
Rosperiwrinkle	Alkali treatment	30.34	(Vinod et al., 2019)
Rice husk	Alkali treatment	50.20	(Johar et al., 2012)
Giant reed	Alkali treatment	67.00	(Suárez et al., 2023)
Banana peel	Alkali treatment	15.75	(Naeem et al., 2022)
Neem tree bark	Water retting	65.04	(Manimaran et al., 2018)
Bamboo	Alkali treatment	22.86	(Abdul Karim et al., 2023)
UTMH	Mechanical milling	48.17	Current work
TMH	Alkali treatment	66.67	Current work

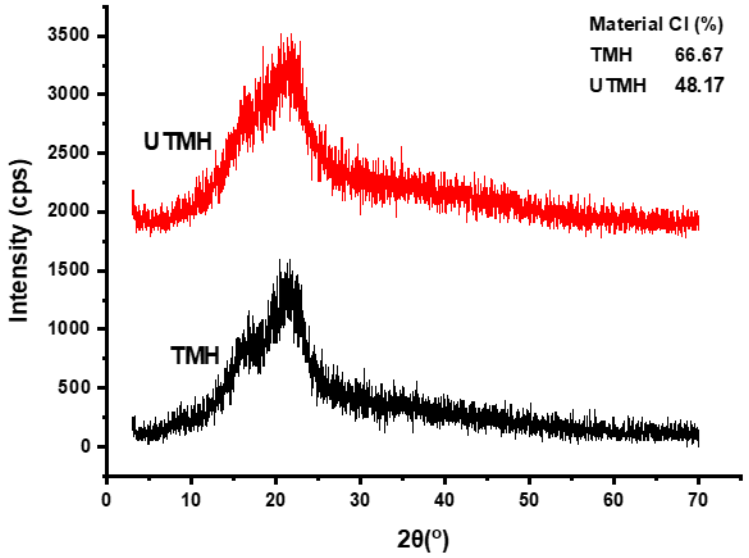

Figure 2: XRD of the Pattern of UTMH and TMH

FTIR Analysis of UTMH and TMH

The functional groups in the UTMH and TMH were investigated using the FTIR spectroscopy approach, as illustrated in Figure 3. The spectra from FTIR spectroscopy are recorded between 4000 and 500 cm^{-1}. The broadband of the spectrum at about 4000-3000 cm^{-1} was described as an alcohol molecule or hydrogen-bonded OH stretching from hemicellulose, cellulose, and lignin (Mushtaq et al., 2023). The wide band at 3400 to 2854 cm^{-1} was found to be caused by the C-H bond frequency observed in alkane groups. The lignin and hemicellulose compounds' strong peak for C=O groups in the ketone and crabenyl groups was displayed as peaks at 1660 to 1655 cm^{-1} and 1650 to 1340 cm^{-1}, respectively (Bouramdane et al., 2022). UTMH and TMH spectra have peaks broadband of 3293 cm^{-1} and 3317 cm^{-1}, respectively, which match the strech vibration of O-H. Similarly, the peaks at 2919 cm^{-1} and 2888 cm^{-1} in the UTMH and TMH spectra, respectively, correspond to pure cellulose's aliphatic saturated C-H stretching vibration. The peak at 1602 cm^{-1} in the UTMH spectra was related to the C=O stretching vibration of acetyl groups in hemicellulose compounds, as illustrated in Figure 3. The disappearance of THM spectra peaks in the broadband range of 1460–1650 cm^{-1} may be the consequence of a drop in hemicellulose concentration, as shown in Figure 3. The peaks at 1512 to 1400 cm^{-1} represent the aromatic structure of lignin found in millet husk. The peak 1512 cm^{-1} appears in the UTMH spectra and seems to decrease for TMH spectra, which is proof of a decrease in lignin content and its removal by treatment with NaOH solution. The peaks in the range of 1512 – 1371 cm^{-1} show O-H stretching of cellulose, C-H bending of hemicellulose, and C-O stretching of the OH group. The peak at 1243 cm^{-1} is attributed to C-H bending of the hemicellulose compound and its removal by 3 % NaOH treatment. Peaks at 1029 cm^{-1} and 1027 cm^{-1} might be attributed to the C-H vibration stretching of the OH group in cellulose, and 898 cm^{-1} to the existence of β-glycosidic connection between the monosacharides on the UTMH spectra (Bekele et al., 2022; Dungani et al., 2024).

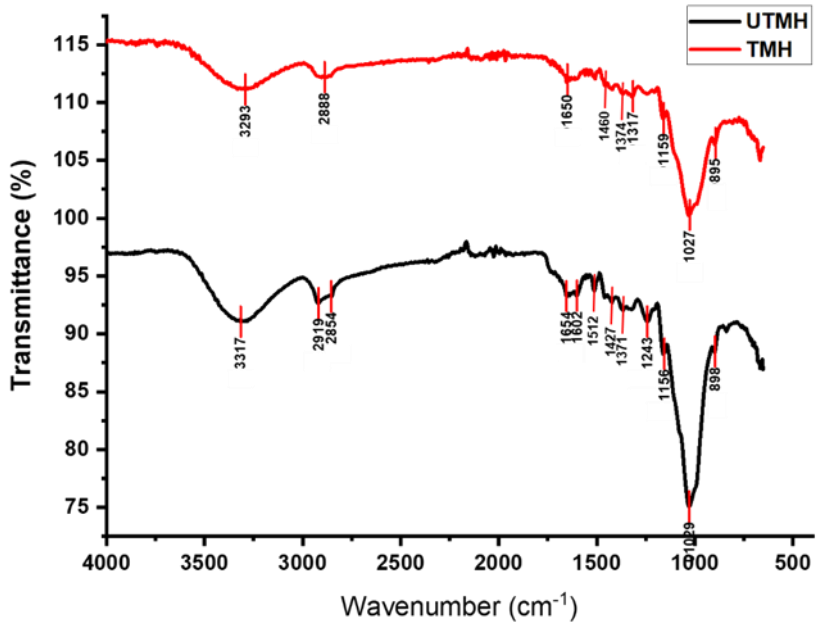

Figure 3: FTIR od UTMH and TMH

TGA and Derivative Thermogravimetry (DTG) Analysis of UTMH and TMH

The TGA and DTG results of the UMTH and TMH are depicted in Figures 4a and 4b, respectively. The weight loss and thermal stability of UTMH and TMH were assessed using the DTG and TGA. The TGA curve of UTMH and TMH is categorized into four stages of weight loss as depicted in Figures 4a and 4b. The first stage experienced slow and linear mass degradation for both UMTH and TMH, and it occurred between 28.60 to 331.71 ˚C. This first stage of breakdown allowed moisture to escape, which was brought about by the structurally integrated and physically absorbed water molecules in the UTMH and TMH (Aliyu et al., 2023; Pokhriyal et al., 2023). The first stage of TGA of UTMH and TMH experienced weight loss of 0.372 mg (0.37 %) and 3.576 mg (3.58 %), respectively. The thermal stability of TMH in the first stage of TGA analysis could be a result of a reduction in hemicellulose content. The second stage of degradation experienced greater degradation than the first stage. The TGA (Figure 4a) of the second stage of UTMH and TMH witness weight losses of 30.49 mg (25.60 %) and 30.51 mg (27.01 %), respectively, between 324.43 to 382.26 ˚C. The second stage of degradation occurred most likely due to the decomposition of organic compounds linked with cellulose, hemicellulose, and lignin (Anuar et al., 2020). The third stage of degradation occurred over a short temperature range from 386.87 to 412.25 ˚C with greater weight loss compared to the second stage. The weight loss in the third stage for UTMH and TMH was 42.78 mg (58.81 %) and 48.60 mg (59.60 %), respectively. The fraction of weight loss of UTMH was lower compared to the TMH, and this could be due to the silica content and lignin present in the UTMH that were not reduced by the alkaline treatment. The higher weight loss experienced with TMH could be due to the reaction severity of NaOH and a decrease in the proportion of heat-stable lignin, which is in accordance with the study of Saadiah et al., (2021). The final stage of degradation was experienced from 502.12 to 888.39 ˚C with weight loss of 2.85 mg (12.01 %) and 6.15 mg (13.02 %) for UTMH and TMH, respectively. The decomposition in the fourth stage could be associated with breakdown of highly cellulose and thermally unstage hemicellulose. The onset of the decomposition of the TMH suggest it possible and potential application as reinforcement for polymer matrix composite production. The DTG curve (Figure 4b) of TMH revealed two pronounced peaks at 147.87 ˚C and 405.58 ˚C both corresponding to the disintergration of cellulose. These peaks are associated with partial the disintegration of cellulose and hemicellulose. The DTG curve of UTMH showed pronouced peaks at 126.50 ˚C and 420.83 ˚C and this could be due to disintegration of lignin and probably the disintegration of long chain cellulose.

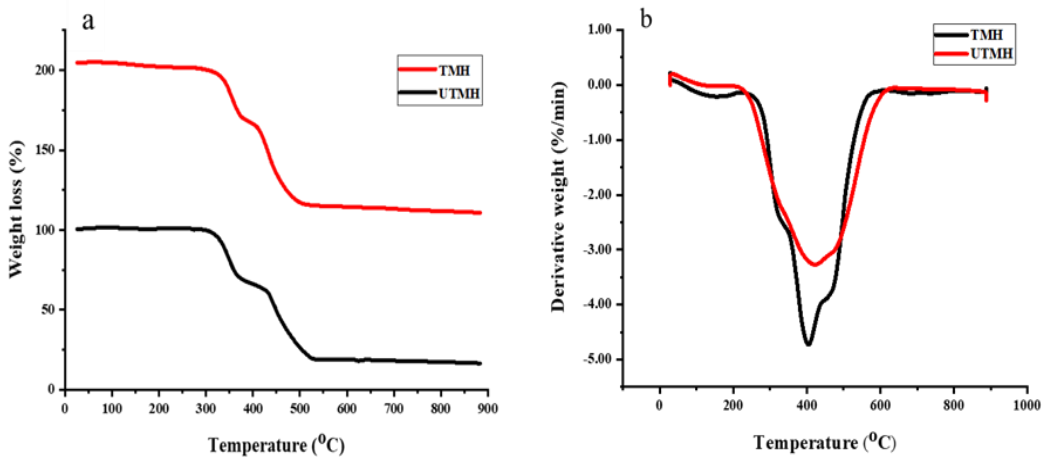

Figure 4. (a) UTMH and TMH TGA curve, and (b) UMTH and TMH DTG curves

Morphology of UTMH and TMH

The scanning electron microscopy was used to examine the surface morphologies of UMTH and TMH at various magnifications of 100 µm, 500 µm, and 1500 µm, as shown in Figure 5. Figures 5(a-c) revealed the surface morphologies of UTMH showing loosely bound debris particles, micro-voids, and a smooth surface that will result in loose bonding with the polymer matrix when employed for composite production. The debris could be lignin and hemicellulose of the surfaces of the UTMH. Figures 5(d-f) showed multiple nano-fibril and flake-shaped particles all over the THM surface. It was thought that the 3 % NaOH solution treatment would remove the lignin and hemicellulose from the millet husk's surface, revealing the flakes and cellulose nano-fibrils. These cellulose nano-fibrils and flakes will be responsible for enhancing wettability when utilized as reinforcement in a polymer matrix, thereby resulting in load transfer between the matrix and reinforcement.

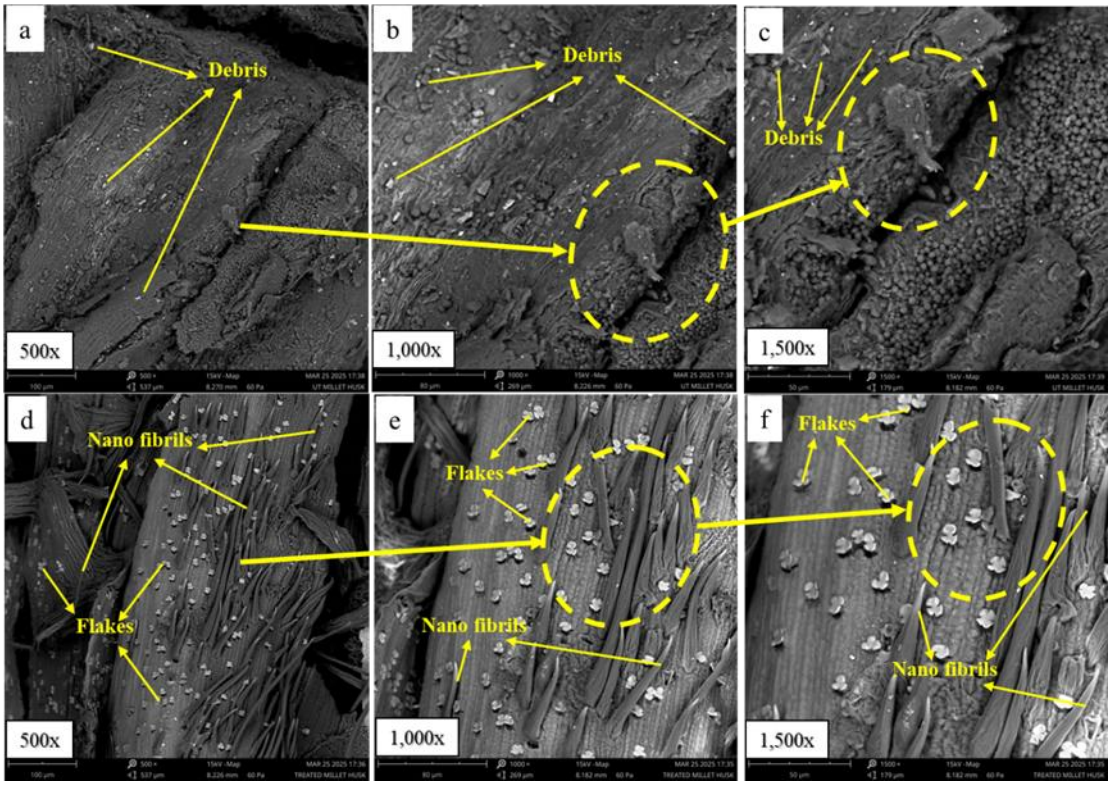

Figure 5: SEM Morphologies of (a) UTMH at 500x, (b) UTMH at 1000x, (c) UTMH at 1500x, (d) TMH at 500x, (e) TMH at 1000x, and (f) TMH at 1500x

CONCLUSION

This work provides a thorough analysis of UTMH and TMH to access their potential applicability as reinforcing materials in polymer composites. The results showed that the TMH has a high cellulose content of 73.47 % and a low density of 0.10 g/cm^3, making it appropriate for the development of high-strength and lightweight polymer composites. Consequently, the moisture contents of TMH and UTMH are 1.37 % and 5.94 %, respectively, which are low enough compared to other natural fibers that have been utilized for the development of polymer composites. The crystallinity index of 66.67 % of TMH was found to be higher than that of sugarcane bagasse.

The TMH surface had a rough morphological appearance with nano-fibrils and flakes due to the removal of lignin, hemicellulose, and debris, allowing for efficient bonding with the polymer matrix. Thus, from the results and analysis carried out, the UTMH and TMH could be economically and potentially viable reinforcing materials for the development of polymer composites.

ACKNOWLEDGEMENT

The authors hereby acknowledge Tertiary Education Trust Fund (TETFUND) as the founding source for this research and Waziri Umaru Federal Polytechnic, Birnin Kebbi, for choosing us as recipients of the TETFUND research grant.

REFERENCES

Abdul Karim, M. R., Tahir, D., Khan, K. I., Hussain, A., Haq, E. U., & Malik, M. S. (2023). Improved mechanical and water absorption properties of epoxy-bamboo long natural fibres composites by eco-friendly Na 2 CO 3 treatment. *Plastics, Rubber and Composites*, *52*(2), 114–127. https://doi.org/10.1080/14658011.2022.2030152

Acharya, P., Pai, D., Bhat, K. S., & Mahesha, G. T. (2024). Effect of Surface Chemical Modifications on Thermo-Physical and Mechanical Properties of Helicteres isora Natural Fiber. *Journal of Natural Fibers*, *21*(1). https://doi.org/10.1080/15440478.2024.2406454

Adamu, B. F., Shitahun, Y., Adane, S., Aferu, T., & Tadesse, K. (2024). Extraction and characterization of bark fibers from Ethiopian Ficus thonningii tree. *Discover Materials*, *4*(1), 1–11. https://doi.org/10.1007/s43939-024-00141-2

Adazabra, A. N., & Viruthagiri, G. (2023). Use of waste husk from millet grain cultivation in the production of fired clay bricks. *International Journal of Ceramic Engineering & Science*, *5*(4). https://doi.org/10.1002/ces2.10179

Al-Maharma, A., & Al-Huniti, N. (2019). Critical Review of the Parameters Affecting the Effectiveness of Moisture Absorption Treatments Used for Natural Composites. *Journal of Composites Science*, *3*(1), 27. https://doi.org/10.3390/jcs3010027

Aliyu, I., Sapuan, S. M., Zainudin, E. S., Rashid, U., Zuhri, M. Y. M., & Yahaya, R. (2023). Characterization of Ash from Sugar Palm [Arenga Pinnata (Wrumb) Merr .] Fiber for Industrial Application. *Journal of Natural Fibers*, *20*(1). https://doi.org/10.1080/15440478.2023.2170943

Anuar, M. F., Fen, Y. W., Zaid, M. H. M., Matori, K. A., & Khaidir, R. E. M. (2020). The Physical and Optical Studies of Crystalline Silica Derived from the Green Synthesis of Coconut Husk Ash. *Applied Sciences*, *10*(6), 2128. https://doi.org/10.3390/app10062128

Atalie, D., & Gideon, R. K. (2018). Extraction and characterization of Ethiopian palm leaf fibers. *Research Journal of Textile and Apparel*, *22*(1), 15–25. https://doi.org/10.1108/RJTA-06-2017-0035

Bachchan, A. A., Das, P. P., & Chaudhary, V. (2022). Effect of moisture absorption on the properties of natural fiber reinforced polymer composites: A review. *Materials Today: Proceedings*, *49*(xxxx), 3403–3408. https://doi.org/10.1016/j.matpr.2021.02.812

Bashir, M., Ibrahim, A., Idi, A., & Abdulmalik, M. (2022). PROXIMATE COMPOSITION, SENSORY EVALUATION AND PRODUCTION OF COOKIES (BISCUIT) FROM FINGER MILLET AND WHEAT FLOUR. *FUDMA JOURNAL OF SCIENCES*, *6*(1), 1–6. https://doi.org/10.33003/fjs-2022-0601-862

Bekele, A. E., Lemu, H. G., & Jiru, M. G. (2022). Experimental study of physical , chemical and mechanical properties of enset and sisal fibers. *Polymer Testing*, *106*(November 2021), 107453. https://doi.org/10.1016/j.polymertesting.2021.107453

Bouramdane, Y., Fellak, S., El Mansouri, F., & Boukir, A. (2022). Impact of Natural Degradation on the Aged Lignocellulose Fibers of Moroccan Cedar Softwood: Structural Elucidation by Infrared Spectroscopy (ATR-FTIR) and X-ray Diffraction (XRD). *Fermentation*, *8*(12), 698. https://doi.org/10.3390/fermentation8120698

Dungani, R., Bakshi, M. I., Hanifa, T. Z., Dewi, M., Syamani, F. A., Mahardika, M., & Fatriasari, W. (2024). Isolation and Characterization of Cellulose Nanofiber (CNF) from Kenaf *(Hibiscus cannabinus)* Bast through the Chemo-Mechanical Process. *Journal of Renewable Materials*, *12*(6), 1057–1069. https://doi.org/10.32604/jrm.2024.049342

Eyupoglu, S., Eyupoglu, C., & Merdan, N. (2024). Physico-chemical characterization of Sambucus ebulus L. plant stem fiber. *Biomass Conversion and Biorefinery*, *14*(17), 20623–20633. https://doi.org/10.1007/s13399-023-04054-7

Gairola, S., Sinha, S., & Singh, I. (2022). Novel millet husk crop-residue based thermoplastic composites: Waste to value creation. *Industrial Crops and Products*, *182*, 114891. https://doi.org/10.1016/j.indcrop.2022.114891

Hamin, S. H., Sayid Abdullah, S. H. Y., Lananan, F., Abdul Hamid, S. H., Kasan, N. A., Mohamed, N. N., & Endut, A. (2023). Effect of chemical treatment on the structural, thermal, and mechanical properties of sugarcane bagasse as filler for starch-based bioplastic. *Journal of Chemical Technology & Biotechnology*, *98*(3), 625–632. https://doi.org/10.1002/jctb.7218

Huang, Y., Meng, F., Liu, R., Yu, Y., & Yu, W. (2019). Morphology and supramolecular structure characterization of cellulose isolated from heat-treated moso bamboo. *Cellulose*, *26*(12), 7067–7078. https://doi.org/10.1007/s10570-019-02614-7

Ibrahim, M. I. J., Sapuan, S. M., Zainudin, E. S., & Zuhri, M. Y. M. (2019). Potential of using multiscale corn husk fiber as reinforcing filler in cornstarch-based biocomposites. *International Journal of Biological Macromolecules*, *139*, 596–604. https://doi.org/10.1016/j.ijbiomac.2019.08.015

Ikumapayi, O. M., Afolalu, S. A., Bodunde, O. P., Ugwuoke, C. P., Benjamin, H. A., & Akinlabi, E. T. (2022). Efficacy of heat treatment on the material properties of aluminium alloy matrix composite impregnated with silver nano particle/calcium carbonate Al –AgNp/CaCO3. *International Journal of Advanced Technology and Engineering Exploration*, *9*(89). https://doi.org/10.19101/IJATEE.2021.874829

Ilyas, R. A., Sapuan, S. M., Asyraf, M. R. M., Dayana, D. A.

Z. N., Amelia, J. J. N., Rani, M. S. A., Norrrahim, M. N. F., Nurazzi, N. M., Aisyah, H. A., Sharma, S., Ishak, M. R., Rafidah, M., & Razman, M. R. (2021). Polymer Composites Filled with Metal Derivatives: A Review of Flame Retardants. *Polymers*, *13*(11), 1701. https://doi.org/10.3390/polym13111701

Ilyas, R. A., Sapuan, S. M., Ishak, M. R., & Zainudin, E. S. (2018). Development and characterization of sugar palm nanocrystalline cellulose reinforced sugar palm starch bionanocomposites. *Carbohydrate Polymers*, *202*(September), 186–202. https://doi.org/10.1016/j.carbpol.2018.09.002

Johar, N., Ahmad, I., & Dufresne, A. (2012). Extraction, preparation and characterization of cellulose fibres and nanocrystals from rice husk. *Industrial Crops and Products*, *37*(1), 93–99. https://doi.org/10.1016/j.indcrop.2011.12.016

Karimah, A., Ridho, M. R., Munawar, S. S., Adi, D. S., Ismadi, Damayanti, R., Subiyanto, B., Fatriasari, W., & Fudholi, A. (2021). A review on natural fibers for development of eco-friendly bio-composite: characteristics, and utilizations. *Journal of Materials Research and Technology*, *13*, 2442–2458. https://doi.org/10.1016/j.jmrt.2021.06.014

Khan, A., Vijay, R., Singaravelu, D. L., Sanjay, M. R., Siengchin, S., Verpoort, F., Alamry, K. A., & Asiri, A. M. (2021). Extraction and characterization of natural fiber from Eleusine indica grass as reinforcement of sustainable fiber reinforced polymer composites. *Journal of Natural Fibers*, *18*(11), 1742–1750. https://doi.org/10.1080/15440478.2019.1697993

Kumar, R., Ul Haq, M. I., Raina, A., & Anand, A. (2019). Industrial applications of natural fibre-reinforced polymer composites – challenges and opportunities. *International Journal of Sustainable Engineering*, *12*(3), 212–220. https://doi.org/10.1080/19397038.2018.1538267

Kusuma, H. S., Permatasari, D., Umar, W. K., & Sharma, S. K. (2024). Sugarcane bagasse as an environmentally friendly composite material to face the sustainable development era. *Biomass Conversion and Biorefinery*, *14*(21), 26693–26706. https://doi.org/10.1007/s13399-023-03764-2

Lee, C. H., Khalina, A., & Lee, S. H. (2021). Importance of Interfacial Adhesion Condition on Characterization of Plant-Fiber-Reinforced Polymer Composites: A Review. *Polymers*, *13*(3), 438. https://doi.org/10.3390/polym13030438

Manimaran, P., Senthamaraikannan, P., Murugananthan, K., & Sanjay, M. R. (2018). Physicochemical Properties of New Cellulosic Fibers from Azadirachta indica Plant. *Journal of Natural Fibers*, *15*(1), 29–38. https://doi.org/10.1080/15440478.2017.1302388

Mohammadi, M., Ishak, M. R., & Sultan, M. T. H. (2024). Exploring Chemical and Physical Advancements in Surface Modification Techniques of Natural Fiber Reinforced Composite: A Comprehensive Review. *Journal of Natural Fibers*, *21*(1). https://doi.org/10.1080/15440478.2024.2408633

Morin, S., Dumoulin, L., Delahaye, L., Jacquet, N., & Richel, A. (2021). Green composites based on thermoplastic starches and various natural plant fibers: Impacting parameters of the mechanical properties using machine-learning. *Polymer Composites*, *42*(7), 3458–3467. https://doi.org/10.1002/pc.26071

Mushtaq, B., Ahmad, F., Nawab, Y., & Ahmad, S. (2023). Optimization of the novel jute retting process to enhance the fiber quality for textile applications. *Heliyon*, *9*(11), e21513. https://doi.org/10.1016/j.heliyon.2023.e21513

Naeem, M. A., Siddiqui, Q., Khan, M. R., Mushtaq, M., Wasim, M., Farooq, A., Naveed, T., & Wei, Q. (2022). Bacterial cellulose-natural fiber composites produced by fibers extracted from banana peel waste. *Journal of Industrial Textiles*, *51*(1_suppl), 990S-1006S. https://doi.org/10.1177/1528083720925848

Paramasivam, A., Kanny, K., Turup Pandurangan, M., & Ramachandran, V. (2024). Mechanical behavior of glass fiber-reinforced hollow glass particles filled epoxy composites under thermal loading. *Journal of Composite Materials*, *58*(18), 2027–2044. https://doi.org/10.1177/00219983241259113

Pokhriyal, M., Kumar, P., Sanjay, R., Rangappa, M., & Siengchin, S. (2023). Effect of alkali treatment on novel natural fiber extracted from Himalayacalamus falconeri culms for polymer composite applications. *Biomass Conversion and Biorefinery*, *0123456789*. https://doi.org/10.1007/s13399-023-03843-4

Rao, H. J., Singh, S., & Janaki Ramulu, P. (2023). Characterization of a Careya Arborea Bast Fiber as Potential Reinforcement for Light Weight Polymer Biodegradable Composites. *Journal of Natural Fibers*, *20*(1), 71–87. https://doi.org/10.1080/15440478.2022.2128147

Rao, H. J., Singh, S., Ramulu, P. J., Suyambulingam, I., Sanjay, M. R., & Siengchin, S. (2024). Isolation and characterization of a novel lignocellulosic fiber from Butea monosperma as a sustainable material for lightweight polymer composite applications. *Biomass Conversion and Biorefinery*, *14*(20), 25317–25329. https://doi.org/10.1007/s13399-023-04631-w

Saadiah, H., Nadia, F., Zhu, J., & Wakisaka, M. (2021). Enhanced crystallinity and thermal properties of cellulose from rice husk using acid hydrolysis treatment. *Carbohydrate Polymers*, *260*(October 2020), 117789. https://doi.org/10.1016/j.carbpol.2021.117789

Samanth, M., & Bhat, K. S. (2023). Sustainable Chemistry for Climate Action Conventional and unconventional chemical treatment methods of natural fibres for sustainable biocomposites. *Sustainable Chemistry for Climate Action*, *3*(February), 100034. https://doi.org/10.1016/j.scca.2023.100034

Sánchez-Safont, E. L., Aldureid, A., Lagarón, J. M., Gámez-Pérez, J., & Cabedo, L. (2018). Biocomposites of different lignocellulosic wastes for sustainable food packaging applications. *Composites Part B: Engineering*, *145*, 215–225. https://doi.org/10.1016/j.compositesb.2018.03.037

Sankhla, S., Sardar, H. H., & Neogi, S. (2021). Greener extraction of highly crystalline and thermally stable cellulose micro-fibers from sugarcane bagasse for cellulose nano-fibrils

preparation. *Carbohydrate Polymers*, *251*(September 2020), 117030. https://doi.org/10.1016/j.carbpol.2020.117030

Sanyang, M. L., Sapuan, S. M., Jawaid, M., Ishak, M. R., & Sahari, J. (2016). Effect of sugar palm-derived cellulose reinforcement on the mechanical and water barrier properties of sugar palm starch biocomposite films. *BioResources*, *11*(2), 4134–4145. https://doi.org/10.15376/biores.11.2.4134-4145

Segal, L., Creely, J. J., Martin, A. E., & Conrad, C. M. (1959). An Empirical Method for Estimating the Degree of Crystallinity of Native Cellulose Using the X-Ray Diffractometer. *Textile Research Journal*, *29*(10), 786–794. https://doi.org/10.1177/004051755902901003

Suárez, L., Barczewski, M., Kosmela, P., Marrero, M. D., & Ortega, Z. (2023). Giant Reed (Arundo donax L.) Fiber Extraction and Characterization for Its Use in Polymer Composites. *Journal of Natural Fibers*, *20*(1), 1–15. https://doi.org/10.1080/15440478.2022.2131687

Tarique, J., Sapuan, S. M., & Khalina, A. (2022). Extraction and Characterization of a Novel Natural Lignocellulosic (Bagasse and Husk) Fibers from Arrowroot (Maranta Arundinacea). *Journal of Natural Fibers*, *19*(15), 9914–9930. https://doi.org/10.1080/15440478.2021.1993418

Thapliyal, D., Verma, S., Sen, P., Kumar, R., Thakur, A., Tiwari, A. K., Singh, D., Verros, G. D., & Arya, R. K. (2023). Natural Fibers Composites: Origin, Importance, Consumption Pattern, and Challenges. *Journal of Composites Science*, *7*(12), 506. https://doi.org/10.3390/jcs7120506

Vinod, A., Vijay, R., Singaravelu, D. L., Sanjay, M. R. R., Siengchin, S., & Moure, M. M. (2019). Characterization of untreated and alkali treated natural fibers extracted from the stem of Catharanthus roseus. *Materials Research Express*, *6*(8), 085406. https://doi.org/10.1088/2053-1591/ab22d9

Wan Nadirah, W. O., Jawaid, M., Al Masri, A. A., Abdul Khalil, H. P. S., Suhaily, S. S., & Mohamed, A. R. (2012). Cell Wall Morphology, Chemical and Thermal Analysis of Cultivated Pineapple Leaf Fibres for Industrial Applications. *Journal of Polymers and the Environment*, *20*(2), 404–411. https://doi.org/10.1007/s10924-011-0380-7

Yousaf, L., Hou, D., Liaqat, H., & Shen, Q. (2021). Millet: A review of its nutritional and functional changes during processing. *Food Research International*, *142*(17), 110197. https://doi.org/10.1016/j.foodres.2021.110197